Revista Brasileira de Ciência do Solo

Division - Soil In Space and Time | Commission - Soil Genesis and Morphology

Technosols of Fundão dam tailings: Chemical and physical properties in the upper riverine landscapes

Pedro Henrique Araújo Almeida[(1)*], Carlos Ernesto Gonçalves Reynaud Schaefer[(1)], Márcio Rocha Francelino[(1)], Anderson Almeida Pacheco[(1)], Eliana Elizabeth dos Santos[(1)], Elpidio Inácio Fernandes Filho[(1)], Anifo Ibraimo[(1)] and José Alexandre Melo Demattê[(2)]

[(1)] Universidade Federal de Viçosa, Departamento de Solos, Viçosa, Minas Gerais, Brasil.
[(2)] Universidade de São Paulo, Escola Superior de Agricultura “Luiz de Queiroz”, Piracicaba, São Paulo, Brasil.

ABSTRACT: Failures of mining tailings dams can cause severe environmental impacts, as sadly illustrated by the Fundão dam collapse in Mariana-Minas Gerais State, Brazil, in 2015. This event induced significant physical and chemical changes in the affected landscape, including variations in soil pH, texture, and key edaphic properties. Soils formed from post-industrial anthropogenic activities, known as Technosols, exhibit high biological, chemical, and physical heterogeneity. In the affected area, Technosols comprise a mixture of tailings, iron mining sediments, natural soils, and debris, with high concentrations of iron oxides, silt, and fine sand. This study aimed to deepen the understanding of Technosols on floodplains and riverbanks impacted by the dam rupture by characterizing their physical and chemical properties in detail. Seventy soil profiles were analyzed — 50 Technosols and 20 unaffected soils — using a slice-wise algorithm to generate standard profile sketches for comparison. Tailings-containing layers exhibit distinct chemical characteristics, including higher pH, phosphorus content, base saturation, and silt content than unaffected layers. These horizons exhibited low cation exchange capacity, indicating low fertility. Tailings deposition was controlled by the basin geomorphological gradient, showing greater heterogeneity upstream and more uniformity downstream. Physically, Technosols displayed higher fine particle content in surface layers, associated with the tailings, while deeper layers showed increased coarse sand and clay, reflecting truncated unaffected horizons of the alluvial environment. Chemically, impacted soils exhibited elevated pH and slight increases in phosphorus, sodium, and potassium at the surface, contrasting with more acidic and less fertile unaffected soils downwards, despite local variability, most profiles showed homogeneous responses, with impacts confined to surface layers.

Keywords: mining dam failure, environmental impacts, geomorphological gradient, alluvial environment.

*** Corresponding author:**
E-mail: phalmeida06@gmail.com

Received: March 07, 2025

Approved: July 31, 2025

How to cite: Almeida PHA, Schaefer CEGR, Francelino MR, Pacheco AA, Santos EE, Fernandes Filho EI, Ibraimo A, Demattê JAM. Technosols of Fundão dam tailings: Chemical and physical properties in the upper riverine landscapes. Rev Bras Cienc Solo. 2026;50nspe1:e0250071.
https://doi.org/10.36783/18069657rbcs20250071

Editors: Marcos Gervasio Pereira.

INTRODUCTION

Mining is a highly relevant economic activity in Brazil, especially in the production of metallic substances. Iron ore, concentrated mainly in the Iron Quadrangle (MG) and in the state of Pará, accounted for approximately 60 % of the mining sector revenue in 2023 (ANM, 2023). The main deposits belong to Banded Iron Formations (BIF), consisting of finely laminated rocks, composed predominantly of iron minerals (hematite, magnetite) and silica, formed by chemical precipitation and modified by diagenetic and metamorphic processes (Spier et al., 2007; Carvalho et al., 2014). The types of ore mined in the country, such as itabirite, hematite and canga, have high iron contents and low levels of impurities undesirable to the steel industry, such as sulfur, aluminum and phosphorus. However, growing international demand, driven mainly by China over the last decade, has led to the exploration of lower-grade deposits, resulting in greater tailings generation, often disposed of in dams.

Tailings generated by iron mining can be in liquid or dry form, depending on the processing method used. In general, they are composed predominantly of quartz with a fine grain size, close to that of fine sand (Guerra et al., 2017). In the Iron Quadrangle, it is common for the tailings to have a high proportion of fine particles (silt and clay), resulting from the grinding and physical and/or magnetic separation stages, in addition to the presence of fine-grained hematite in the deposits (Andrade, 2014). The main minerals associated with the tailings include kaolinite, gibbsite, goethite, hematite, magnetite and quartz (Wolff, 2009).

In the last 20 years, three major tailings dam failures have occurred in Minas Gerais, with the most notable disasters being Cataguases (2003), Mariana (2015), and Brumadinho (2019). The Fundão dam failure in Mariana, considered the country's largest environmental disaster, caused human losses and severe impacts on the river plains of the Gualaxo do Norte and Carmo rivers (Marta-Almeida et al., 2016; Segura et al., 2016; Carmo et al., 2017). Such changes compromised agricultural use and the recovery of native vegetation in impacted areas (Duarte et al., 2021; Silva, 2021; Villa, 2022).

Soils developed from material introduced into the environment by human activities are classified as “Technosols” (IUSS Working Group WRB, 2015). In the region affected by the Fundão dam, the Technosol consists of a mixture of iron mining waste and sediments, soils and debris from the affected areas (Schaefer et al., 2015, 2016). According to these authors, this material has a high concentration of iron oxides, silt and fine sand, and, when deposited on the banks, it has altered the surface layers of the soil, causing compaction and surface sealing of the soil and an increase in pH, associated with the use of NaOH in ore processing (Schaefer et al., 2015; Santos, 2019), revealing little physical and morphological variability (Guerra et al., 2017). However, since it is a territorially extensive affected area, it is expected to find different environments throughout the river landscape, with geomorphology, vegetation cover in the surroundings, management actions, and impact mitigation being key aspects in restoring the quality of these Technosols.

In this sense, this study aimed to deepen knowledge of the Technosols formed on floodplains and areas marginal to watercourses directly affected by the Fundão dam tailings, in order to broaden understanding of the incident pedogenetic processes, based on the characterization of their physical and chemical properties.

MATERIALS AND METHODS

Study area

This study was conducted in the Rio Doce Basin, located in areas severely affected by the deposition of tailings from the Fundão Dam, forming a Tecnosol (Figure 1). This event resulted in a heterogeneous mixture of tailings, soils, channel sediments and water that broke through and flowed down the main watercourses, including the Santarém Stream, the Gualaxo do Norte, Carmo and Doce Rivers, and was partially dammed in the upstream sector, above the Risoleta Neves Reservoir.

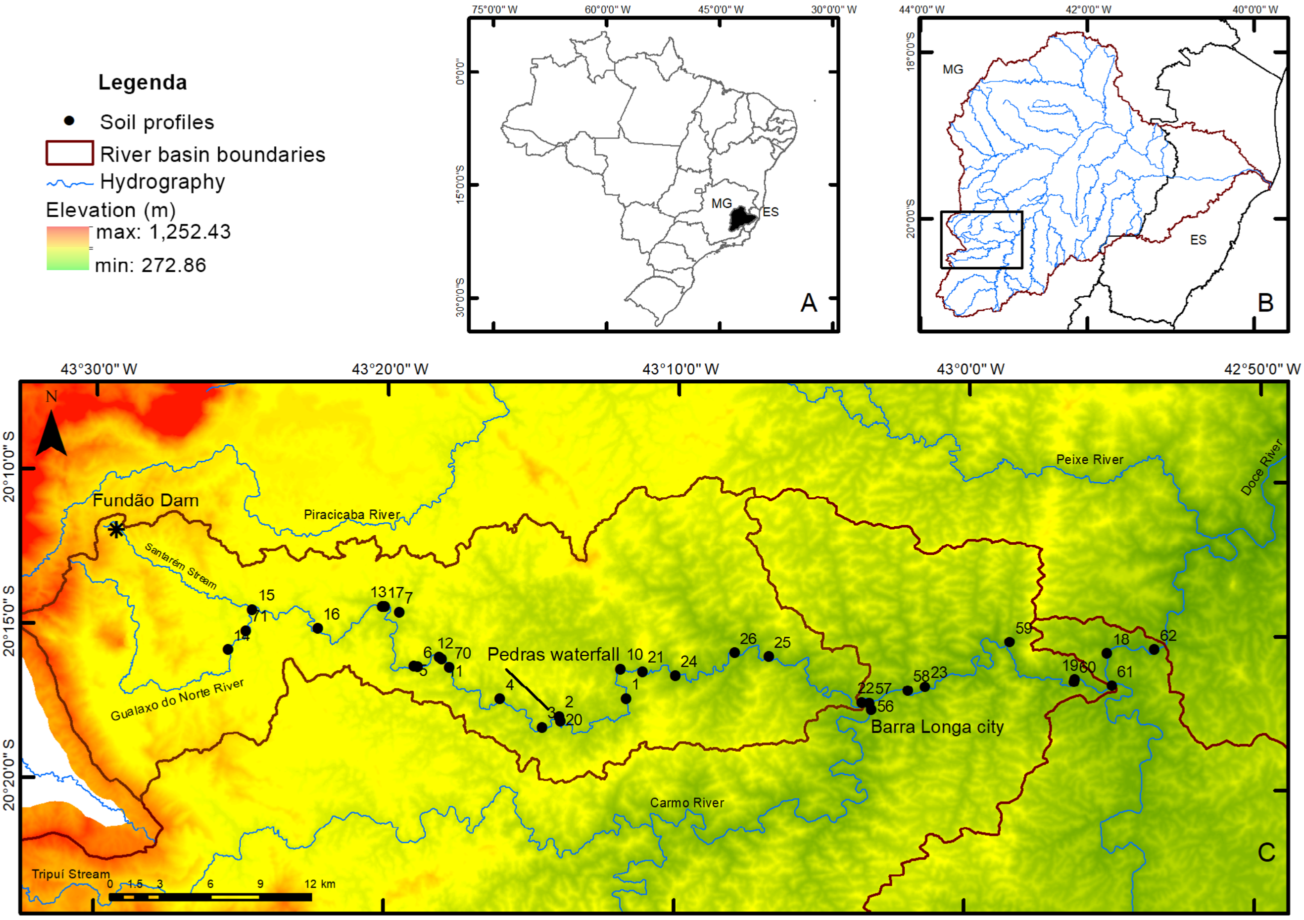

Figure 1. Doce River Basin in Brazil (a), study area within the basin (b), and sample locations along the study area (c).

In this region, the climate is tropical rainy with dry winters, classified as Aw (Köppen, 1948). Gualaxo do Norte and Carmo River Basins are located in the east-southeast region of the Iron Quadrangle and present a predominance of Proterozoic rocks rich in Fe and Au mineralization. The tectonic setting of the QF allowed the formation of several mineral deposits due to the different phases of deformation. In this region, the upper course geological units include rocks from the Minas Supergroup and its subdivisions, which correspond to a succession of Paleoproterozoic sedimentary rocks of high mining interest. Its main units include formations with quartzites, phyllites, itabirites, metaconglomerates and carbonates, representing varied depositional environments, from fluvial and deltaic to shallow marine. Among the main lithological groups, the itabirites of the Cauê Formation, the metaconglomerates of the Moeda Formation and the quartzites of the Caraça Formation stand out, which have both geological and economic importance, especially in relation to iron deposits. The geological units of the middle and lower reaches include the Santa Bárbara Metamorphic Complex, the Acaiaca Metamorphic Complex, the Mantiqueira Metamorphic Complex and the Rio das Velhas Supergroup (Dorr II et al., 1957; Gair, 1958; Dorr II, 1969; Renger et al., 1994). In the upper part of the basin, a steeply sloped mountainous landscape is observed, typical of the Iron Quadrangle, with Cambisols (*Cambissolos*) and Leptosols (*Neossolos*) of highlands, with grassy to shrubby vegetation. Further down in the landscape, elevated plateaus with Petric Plithosols on ferruginous ironstones (Canga) are observed, where Fe mining is underway. In the transition region to the lowlands of the basin, there is a region of aligned ridges, transitional forests, with a predominance of dystrophic Cambisols over acidic phyllites rich in Al. In the lower elevations of the basin, where crystalline basement rocks occur, the *Mares de Morros* predominate, with a predominance of Ferralsols (*Latossolos*) and Acrisols (*Argissolos*) on saprolites, originally covered by Semideciduous Seasonal Forest, mostly replaced by pastures and agricultural areas. In the river plain, natural alluvial soils (Fluvisols/*Neossolos Flúvicos* and Cambisols, in addition to Gleysols/*Gleissolos*) occur in low-energy lacustrine environments with poor drainage. These soils were partially truncated and buried by the wave of tailings, forming the current Technosols under study. In this sector, the Technosols cover an area of approximately 2,200 ha. It is worth noting that in the affected area, environmental restoration measures were implemented, including the removal of waste from the main tributaries' channels, the reconstruction and stabilization of their banks to prevent erosion, and the planting of native species along the river banks.

General characteristics of the soils investigated

This study used a large database of chemical, physical, and morphological properties from 50 soil profiles, collected in areas affected by tailings, as well as 20 reference profiles located adjacent to the impacted area. These soil profiles were described in situ by Schaefer et al. (2016), Santos (2019), and Fundação Renova database, using the classical pedological approach (Santos et al., 2013). Samples were collected by pedogenetic horizon, focusing mainly on texture, structure, and color, which facilitated differentiation of soil horizons, particularly in terms of the presence or absence of tailings. The studied soil profiles ranged in depth from 0.30 to 1.80 m, with an average depth of 0.90 m, considering the entire dataset. Additionally, five samples from fresh tailings deposits, collected 5 days after deposition, were used as time-zero reference material. The physical properties analyzed in this study were: soil depth, granulometric distribution (% coarse sand, % fine sand, % silt, % clay); and chemical properties: pH in water, pH in KCl, P (mg dm^{-3}), K (mg dm^{-3}), Sum of bases (SB) ($cmol_c$ dm^{-3}), Base saturation (%) and organic matter (g kg^{-1}). On soil characterization, pH(H_2O) was determined in the soil:water ratio 1:2.5 (Teixeira et al., 2017). Saturation paste extract (USSL Staff, 1954) was prepared to measure pH and to determine soluble cations (Na^+, K^+, Ca^{2+}, Mg^{2+}). Exchangeable cations were extracted by ammonium acetate (1.0 mol L^{-1}); cation exchange capacity (CEC) was determined by the sodium acetate/ammonium acetate method (USSL Staff, 1954). Soluble and exchangeable Ca^{2+} and Mg^{2+} contents were measured by atomic absorption spectrophotometry, and Na^+ and K^+ by flame emission photometry. Phosphorus content in the soil was extracted by Mehlich-1 (Mehlich, 1978). The P-rem was obtained by Alvarez V et al. (2000). Total organic carbon (TOC) was determined by the wet oxidation method (Mendonça and Matos, 2005).

Data preparation

Using Geographic Information System software, the soil profiles were related to information about the relief and distance from the Fundão dam. Using this information, three groups were grouped according to the fluvial geomorphological sectors described by Felippe and Mendes (2022) *apud* Saadi and Campos (2015), and Oliveira et al. (2017).

According to these authors, the river channels in the mountainous region have rocky and semi-confined beds with a gradual transition to alluvial beds in unconfined valleys. The plains are narrow, with some segments presenting rapids due to the exposed rocky substrate. There are narrow and enclosed valleys with a high slope, explaining high-energy stretches even in the region near the Pedras waterfall. From this stretch to the lower third of the Carmo River, the conditions of the channels change and the valley bottom becomes wider. Throughout the studied area, there are several types of river valleys, including canyons, confined, narrow valleys, wide valleys with small plains, and wide valleys with extensive plains, with smooth to flat profiles.

Hydrogeomorphological sector 1 was delimited from the most upstream point of the basin impacted by the mud. The first profile described in this area is located near the end point of the area impacted by the tailings, characterized by the "rebound" of the mud. This event caused the river flow to change and was caused by the confinement of the Gualaxo do Norte River near its confluence with the Santarém Stream. From this point, the section follows the bed of the main river course to the Pedras Waterfall, located in the district of the same name. Hydrogeomorphological sector 2 begins at this waterfall and continues until the confluence with the Carmo River, in Barra Longa-MG. Hydrogeomorphological sector 3 begins at this point and extends to the confluence with the Piranga River, where the Doce River forms.

To assess the effect of geoforms on the distinction of the sections more clearly, the classification of relief forms proposed by Weiss (2001) was applied, with the aim of evaluating the predominance of the main features. According to Jenny (1994), soil formation is closely related to several factors, and relief and topography are among them. Relief influences soil formation in several ways, including erosion in areas with sloping topography, accumulation of sediments in flatter areas, soil drainage, exposure to climatic elements, and others.

There is an increase in the contribution of the plain areas as the mud travels through the affected sections (Figure 2). On the other hand, there is a reduction in areas where the river flows in a more embedded manner, characterized by slope drainage classes and deeply incised streams. In addition to the spatial effect, the influence of technogenic materials in relation to natural material was evaluated, with a comparative analysis being carried out with soil profiles described outside the impacted area, located in the same study region.

Statistical evaluation

Statistical procedures were performed using scripts and packages developed in the software (R Development Core Team, 2021). To assess the chemical and physical properties of soil profiles at depth, tools from the AQP package developed by Beaudette et al. (2013) were used. The AQP is a specific package for analyzing soil variability based on soil profiles. The analysis was based on an algorithm that constructs soil depth functions, allowing the prediction of central trends, calculation of statistics, and reconstruction of data into a representative depth function (Pinheiro et al., 2016, 2018). The slice-wise algorithm assumes that a representative function for the variation in soil properties with depth can be generated from a collection of profile data, summarized into depth intervals. For this study, the layers 0.00-0.05, 0.05-0.15, 0.15-0.30, 0.30-0.60, 0.60-1.00, and 1.00-2.00 m were adopted. The spline function was then applied to calculate the mean and median for each layer. The spline function is a non-parametric technique suitable for modeling soil properties, adjusting the data for each layer, and maintaining the mean of the soil property (Pinheiro et al., 2016).

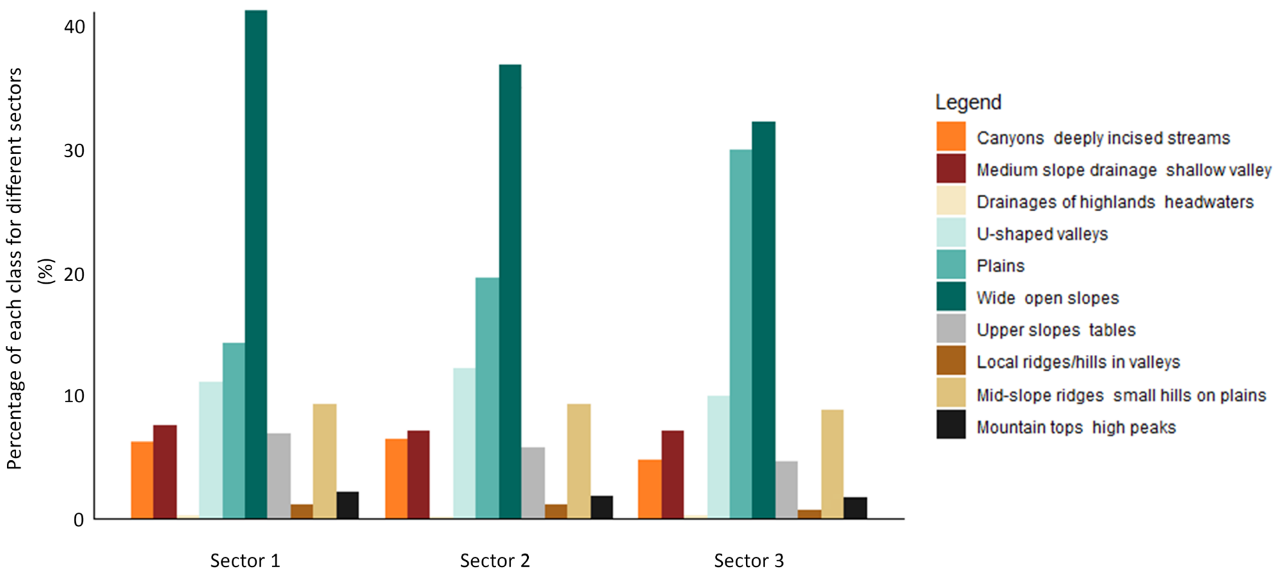

Figure 2. Distribution of landform classes proposed by Weiss (2001) across the study sectors.

To evaluate soil properties that could be used to categorize the data, the variables were subjected to Spearman correlation tests (p=0.05) using the "corrplot" package (Wei et al., 2021), and subsequently, principal component analysis (PCA) and cluster analysis were performed using the "sharpshootR" package (Beaudette et al., 2023) and "FactoMineR" (Husson et al., 2017). Principal Component Analysis (PCA) is a statistical technique used to explore and summarize the variation present in a multivariate dataset. It is often used to analyze environmental data, enabling the identification of non-obvious patterns and relationships among variables, reducing data dimensionality, and facilitating visualization. (Hongyu et al., 2016). The similarity of soil profiles was assessed by comparing the main soil properties at each centimeter of layer, considering the variability of soil properties and the thickness of the diagnostic horizon. The maximum evaluation depth was considered to be the layer that represented at least 70 % of data representativeness. Statistical differences between groups were assessed using the Kruskal-Wallis test, at a 5 % significance level, followed by Dunn's test for multiple comparison between groups.

RESULTS

Description according to AQP(Algorithms for Quantitative Pedology)

When evaluating the groups according to their position in the landscape (Figure 3), in hydrogeomorphological sector 1 (High), the thickness of the tailings layer varied between 0.13 and 1.15 m, with an average of 0.55 m and a standard deviation of 30.08. The thickness of the tailings in sector 2 varied between 0.30 and 0.88 m, with an average of 0.6042 m and a standard deviation of 19.61. In sector 3, the thickness ranged from 0.13 to 1.08 m, with an average of 0.787 m. The lowest standard deviation (18.59) was observed in this sector.

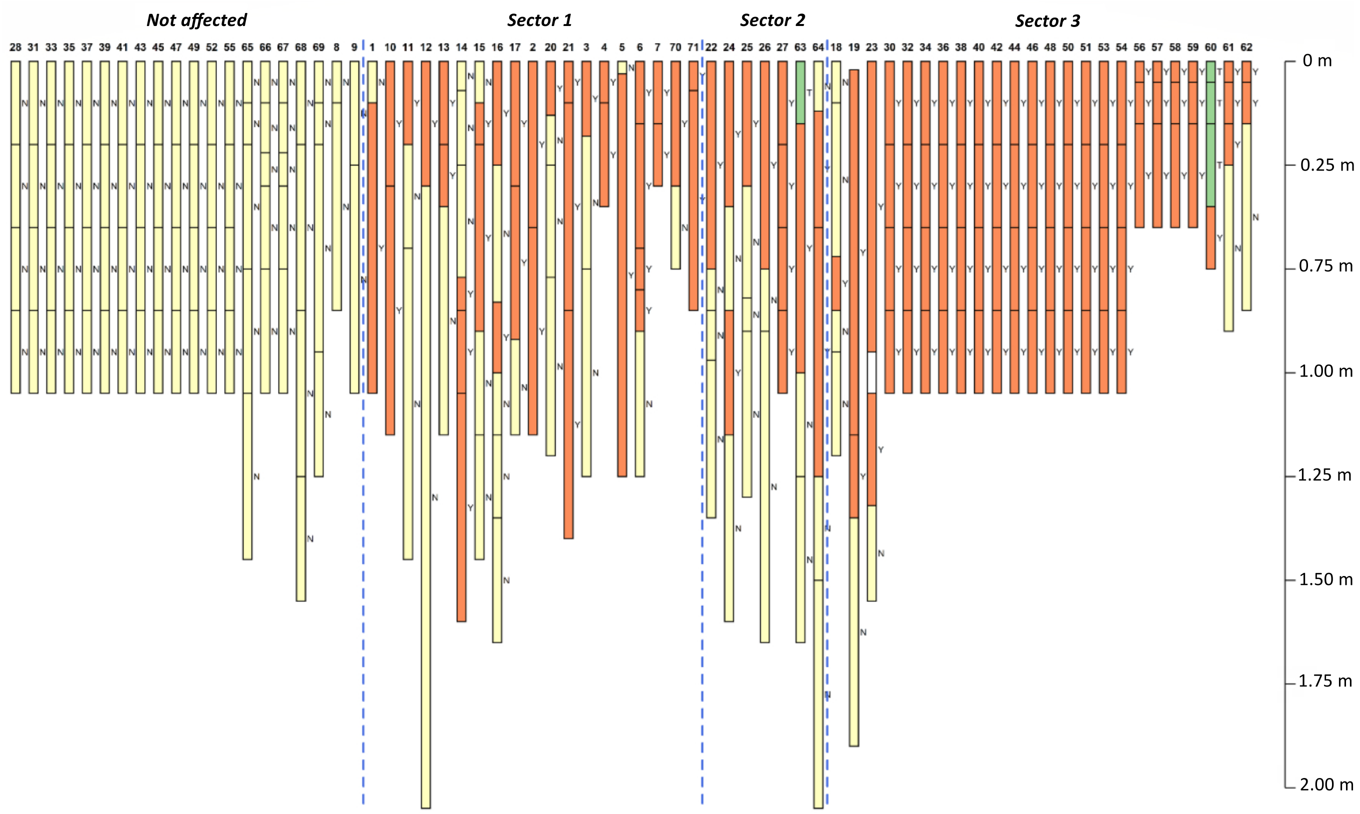

Figure 3. Evaluated soil profiles by sector, with indication of affected layers (orange), unaffected soil layers (yellow), and topsoil (green). Profiles are shown with depth to illustrate the vertical distribution of tailings across sectors of the Gualaxo do Norte River valley.

The three groups showed similar physical signatures, including a predominance of silt and fine sand (Figure 4). In general, similar values were observed in depth in the three groups studied, without identifying any spatial influence on the granulometric distribution of the analyzed soils. However, profiles from group 3 presented greater variability in the contents of coarse sand, silt and clay. For groups 1 and 2, a tendency towards higher clay and coarse sand contents was identified in the deeper layers, related to the presence of layers of natural soil.

A progressive increase in the coarse sand contents was observed in the 0.05-0.15 m layer, accompanying the increasing distance in relation to the breaking point. The observed medians were 76 g kg^{-1} in sector 1, 70 g kg^{-1} in sector 2, and 130 g kg^{-1} in sector 3. The 25th and 75th percentiles ranged from 40 to 103 g kg^{-1} in sector 1, 45 to 170 g kg^{-1} in sector 2 and 70 to 220 g kg^{-1} in sector 3, indicating greater granulometric variability in the sectors furthest from the impact source. Regarding the clay fraction, the medians also indicated an increase along the plain, with 102 g kg^{-1} in sector 192 g kg^{-1} in sector 2 and 120 g kg^{-1} in sector 3. The 25th and 75th percentiles were, respectively, 90 and 124 g kg^{-1} (sector 1), 70 and 130 g kg^{-1} (sector 2) and 89.75 and 200 g kg^{-1} (sector 3).

Considering all samples collected in the profiles, the median pH values were similar among the evaluated groups, ranging from 6.53 to 6.79. According to the classification of Alvarez et al. (1999), these soils range from weakly acidic to weakly alkaline. Phosphorus (P) levels also showed little variation, ranging from 5.4 to 5.9 mg dm^{-3}. On the other hand, potassium (K) and sodium (Na) levels were higher in the soils of group 2, which resulted in a higher base saturation (75.05 %) in this group. Despite the low levels of calcium (Ca^{2+}), magnesium (Mg^{2+}) and organic matter (OM) observed in the evaluated soils, the soils of group 3 presented higher median values of these properties, which contributed to the higher values of sum of bases (SB), effective exchange capacity (t) and total exchange capacity (T) in this group. For soils in group 3, the median value of $Ca^{2+} + Mg^{2+}$ was 1.65 $cmol_c$ dm^{-3}, while the median organic matter reached 0.81 %.

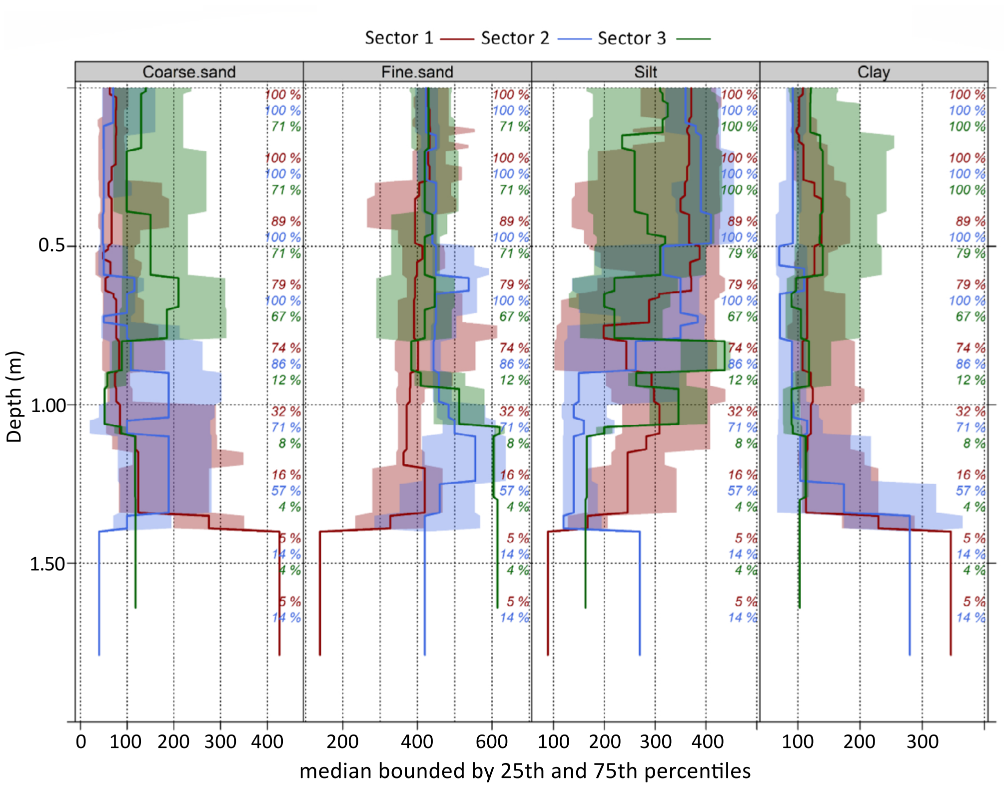

Figure 4. Median values of physical properties for the three Technosol groups under investigation. Red represents profiles from Sector 1 (High), blue from Sector 2 (Medium), and green from Sector 3 (Low).

Tables 1, 2 and 3 show the median values of the chemical properties obtained for the different depths. In general, higher concentrations of phosphorus (P), potassium (K), and organic matter (OM) were observed in the soil surface layers, regardless of the group evaluated. These properties showed a tendency to decrease with increasing depth, with the highest values recorded in the layers between 0.00 and 0.30 m. In group 1 (Table 1), the median values of the chemical properties indicate a decline in fertility with depth. The surface layer (0.00–0.05 m) presented higher pH (6.08), phosphorus (4.4 mg kg^{-1}), potassium (23 mg kg^{-1}), base saturation (V = 55.6 %) and organic matter (6.7 g kg^{-1}). Between 0.05 and 0.30 m, pH and V increased slightly, while P, K and OM decreased. Below 0.30 m, fertility indicators reduced more sharply, with the lowest values observed in the 1.00-2.00 m layer (pH 5.78; P 1.0 mg kg^{-1}; K 1 mg kg^{-1}; V 42.7 %; MO 4.0 g kg^{-1}).

The median values of the soils in Group 2 (Table 2) indicate relative chemical uniformity in the surface layers (0.00–0.15 m), with pH 6.28, P 5.4 mg dm^{-3} and K 25 mg dm^{-3}. Between 0.15 and 0.60 m, the pH increased to 6.76, and base saturation rose from 77.6 to 85 %, despite reductions in K and P stability. Organic matter showed low values throughout the profile and was absent below 0.30 m. In the deeper layers (0.60–2.00 m), a decrease in fertility indicators was observed: pH decreased to 5.87, P and K fell to 0.6 and 16 mg dm^{-3}, respectively, and V to 53.9 %.

Soils in Group 3 showed greater fertility in the surface layers, with pH between 6.6 and 6.8, high levels of phosphorus (6.8 mg dm^{-3}) and potassium (50 mg dm^{-3}), and the highest organic matter content (0.94 %) at 0.00–0.05 m. A gradual reduction in K and OM with depth was observed, while pH remained relatively stable. Between 0.60-1.00 m, K fell to 13 mg dm^{-3}, with moderate V (57.1 %) and OM of 6.7 g kg^{-1}. In the deepest layer (1.00–2.00 m), pH increased to 7.0 and base saturation reached its peak (88.3 %), despite the lower OM (4.0 g kg^{-1}) and lower levels of P (5 mg dm^{-3}) and K (9 mg dm^{-3}), in addition to a significant increase in SB and t (3.76 cmol$_c$ dm^{-3}). Figure 5 presents the graphical representation of the results for the three groups evaluated.

Comparison between the Technosols and non-affected soils

To characterize the physical and chemical properties of the Technosols, standardized sketches of the soils studied were developed, following the methodology of Beaudette et al. (2013), to highlight the variability of soil types (Technosols × Soils from unaffected areas).

The set of unaffected soil samples is composed mostly of profiles of Ferralsols (Latossolos), Cambisols (Cambissolos), and Acrisols (Argissolos), as described in the region near the affected areas. Although these soil classes are in a different position from the vast majority of Technosols, they can occur in the affected area, as evidenced by the presence of hillside areas. Thus, these classes serve as a reference for hillside soils and other soil types that are not located on plains, that is, soils other than Fluvisols (Neossolos Flúvicos) and Cambisols (Cambissolos Flúvicos).

Table 1. Median chemical properties values across soil layers for Group 1 soils

Layer	pH(H_2O)	P	K	SB	t	V	MO
m	-	mg dm^{-3}		cmol$_c$ dm^{-3}		%	g kg^{-1}
0.00-0.05	6.08	4.4	23	1.40	1.40	55.6	6.7
0.05-0.15	6.26	4.9	14	1.35	1.35	58.2	3.9
0.15-0.30	6.52	5.1	10	1.18	1.18	65.8	3.9
0.30-0.60	6.54	2.3	8	1.18	1.26	72.0	3.9
0.60-1.00	6.53	2.7	5	0.99	1.01	54.5	2.7
1.00-2.00	5.78	1.0	1	0.82	0.82	42.7	4.0

pH(H_2O); P: available phosphorus (mg dm^{-3}); K: exchangeable potassium (mg dm^{-3}); SB: sum of bases (cmol$_c$ dm^{-3}); t: effective cation exchange capacity (cmol$_c$ dm^{-3}); V: base saturation (%); MO: organic matter (g kg^{-1}).

Table 2. Median chemical properties values across soil layers for Group 2 soils

Layer	pH (H_2O)	P	K	SB	t	V	MO
m	-	mg dm^{-3}		cmol$_c$ dm^{-3}		%	g kg^{-1}
0.00-0.05	6.28	5.4	25	1.04	1.14	60.4	1.3
0.05-0.15	6.28	5.4	25	1.04	1.14	60.4	1.3
0.15-0.30	6.74	5.6	21	1.29	1.29	77.6	1.3
0.30-0.60	6.76	5.1	17	1.53	1.53	85.0	0
0.60-1.00	6.26	2.1	17	1.61	1.61	64.8	0
1.00-2.00	5.87	0.6	16	1.17	1.17	53.9	0

pH(H_2O); P: available phosphorus (mg dm^{-3}); K: exchangeable potassium (mg dm^{-3}); SB: sum of bases (cmol$_c$ dm^{-3}); t: effective cation exchange capacity (cmol$_c$ dm^{-3}); V: base saturation (%); MO: organic matter (g kg^{-1}).

Table 3. Median chemical parameter values across soil layer intervals for Group 3 soils

Layer	pH (H_2O)	P	K	SB	t	V	MO
m	-	mg dm^{-3}		cmol$_c$ dm^{-3}		%	g kg^{-1}
0.00-0.05	6.6	6.8	50.0	1.21	1.82	58.2	9.4
0.05-0.15	6.7	6.0	39.0	1.18	1.63	58.2	6.7
0.15-0.30	6.8	5.8	22.5	1.27	1.78	55.6	6.7
0.30-0.60	6.6	4.7	20.0	1.61	1.82	53.6	8.1
0.60-1.00	6.6	5.4	13.0	1.63	1.82	57.1	6.7
1.00-2.00	7.0	5.0	9.0	3.76	3.76	88.3	4.0

pH(H_2O); P: available phosphorus (mg dm^{-3}); K: exchangeable potassium (mg dm^{-3}); SB: sum of bases (cmol$_c$ dm^{-3}); t: effective cation exchange capacity (cmol$_c$ dm^{-3}); V: base saturation (%); MO: organic matter (g kg^{-1}).

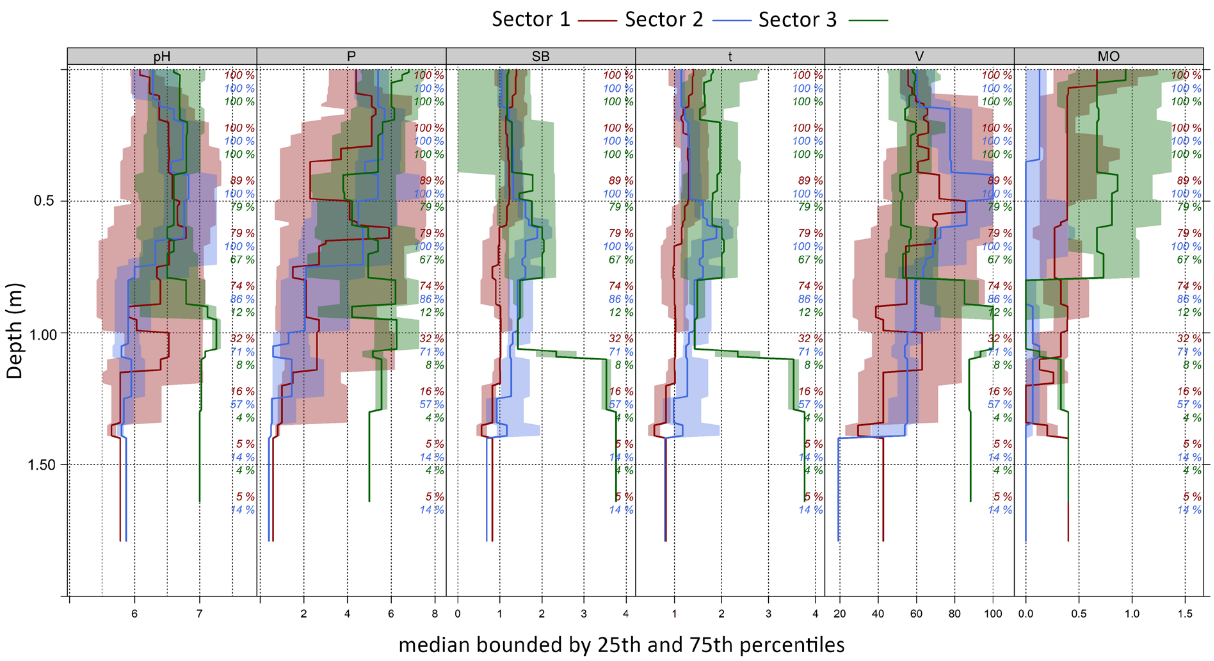

Figure 5. Median values of chemical properties for the three Technosol groups under investigation. Red: profiles from Sector 1 (High); blue: profiles from Sector 2 (Medium); and green: profiles from Sector 3 (Low).

Table 4, figure 6 and figure 7 show the median values of the physical and chemical properties of Technosols at different layers, obtained using the slice-wise algorithm, obtained from the harmonization of the layers for depths recommended by the GlobalSoilMap Project (Arrouays et al., 2014).

Granulometric analysis of the soil profile at depth for Technosols revealed significant variations in the distribution of granulometric fractions with depth. The fine sand and silt fractions present the highest contents in the surface layers, with values close to 441.4-442.4 g kg^{-1} for fine sand and 365.2 g kg^{-1} for silt in the first 0.15 m, remaining relatively constant up to 0.30 m. Coarse sand, in turn, presents lower values in the surface layers (86.4 g kg^{-1} in the 0.00-0.05 m layer) and increases progressively with depth, reaching 143.2 g kg^{-1} in the 1.00-2.00 m layer. The silt fraction decreases continuously with depth, from 365.2 g kg^{-1} in the first 0.15 m to 203.9 g kg^{-1} in the deepest layer (1.00-2.00 m). Clay, although with smaller variations, shows a slight tendency to increase in the intermediate and deep layers, with values ranging from 107 g kg^{-1} at the surface to 143.2 g kg^{-1} in the deepest layer.

Table 4. Median chemical and physical properties values across soil layers for Technosols

Layer	pH	P	K	SB	t	V	MO	Coarse sand	Fine sand	Silt	Clay
m	-	mg dm^{-3}		$cmol_c$ dm^{-3}		%	g kg^{-1}	g kg^{-1}			
0.00-0.05	6.38	5.1	29	1.23	1.45	57.7	6.7	86.4	441.4	365.2	107.0
0.05-0.15	6.52	5.3	22	1.22	1.32	58.8	4.0	85.4	442.4	365.2	107.0
0.15-0.30	6.58	5.4	18	1.22	1.45	63.0	4.0	79.4	442.5	363.6	114.5
0.30-0.60	6.6	4.7	15	1.26	1.53	60.8	4.0	92.5	439.7	343.0	124.8
0.60-1.00	6.34	3.0	12	1.24	1.26	58.2	3.9	107.4	465.1	309.3	118.2
1.00-2.00	5.87	1.0	11	1.02	1.02	53.9	1.3	143.2	509.7	203.9	143.2

$pH(H_2O)$; P: available phosphorus (mg dm^{-3}); K: exchangeable potassium (mg dm^{-3}); SB: sum of bases ($cmol_c$ dm^{-3}); t: effective cation exchange capacity ($cmol_c$ dm^{-3}); V: base saturation (%); MO: organic matter (g kg^{-1}).

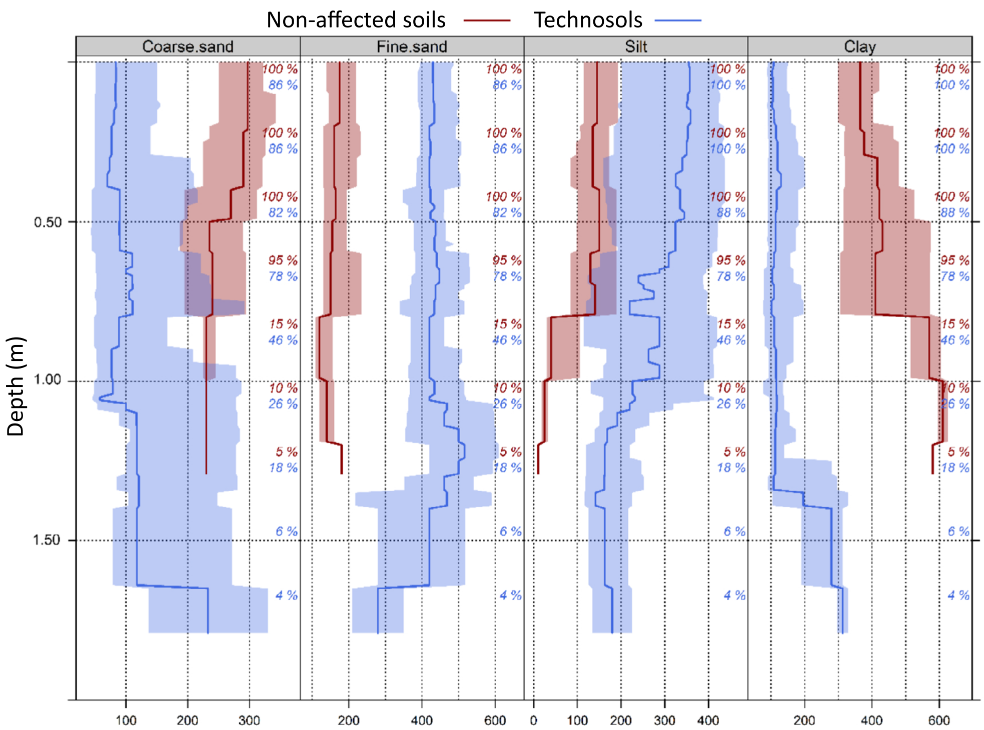

Figure 6. Coarse sand, fine sand, silt, and clay (g kg^{-1}) for the evaluated groups. The percentage value indicates the relative number of soil samples that contributed to the estimate of each variable.

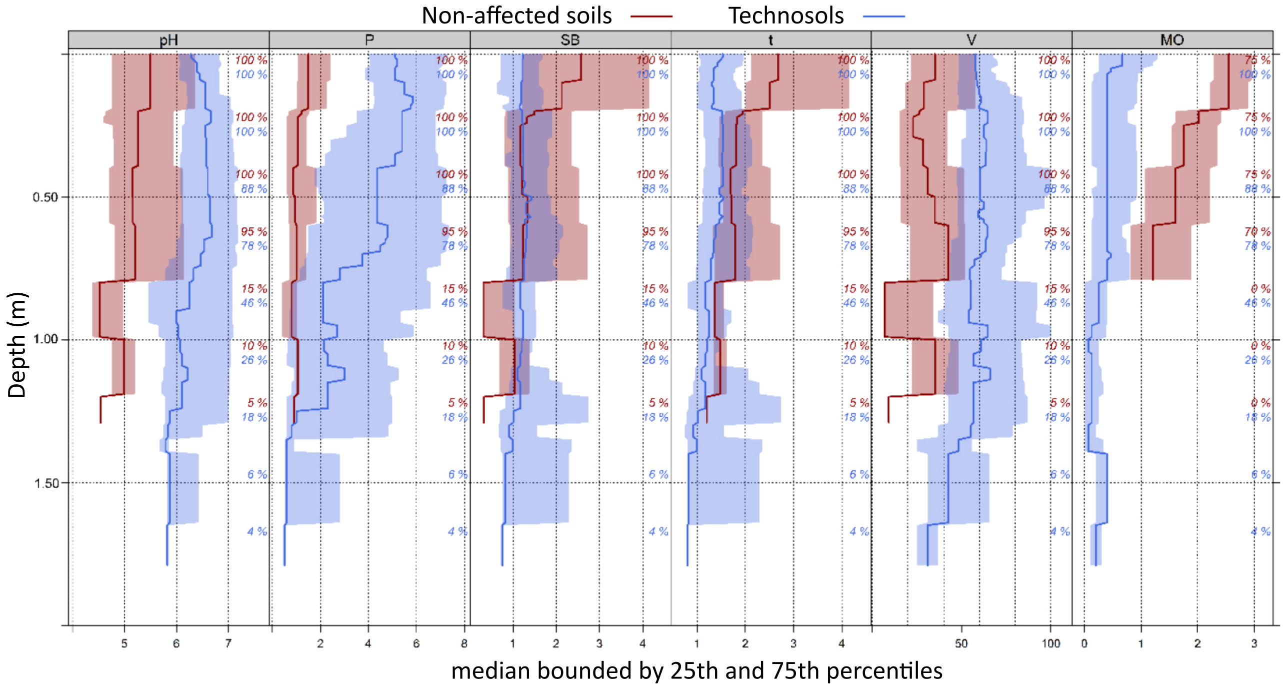

Figure 7. Phosphorous (mg dm^{-3}), pH, sum of bases (SB) (cmol$_c$ dm^{-3}), CEC (cmol$_c$ dm^{-3}), V (%) and organic matter (%). Percent value indicates the relative number of soils that contributed to this variable estimate.

Chemical analysis at depth revealed gradual variations in the properties throughout the profile. The pH(H_2O) showed relatively stable values in the surface layers, varying between 6.38 and 6.6 up to 0.60 m, indicating a slightly acidic to neutral reaction. From 0.60 m onwards, a tendency towards acidification is observed, with the pH decreasing to 6.34 in the 0.60-1.00 m layer and reaching 5.87 at a depth of 1.00-2.00 m. Available phosphorus (P) levels were low throughout the profile, with the highest values observed in the surface layers (5.1 to 5.4 mg dm^{-3} up to 0.30 m), followed by a gradual decrease to 1 mg dm^{-3} in the 1.00-2.00 m layer. This behavior reflects the natural limitation of phosphorus in tropical soils, aggravated by fixation at depth.

Potassium (K) showed a progressive reduction with depth, starting from 29 mg dm^{-3} at the surface to 11 mg dm^{-3} between 1.00-2.00 m. Sum of bases (SB) remained relatively constant up to 0.60 m (~1.2–1.26 cmol$_c$ dm^{-3}), with a slight reduction at greater depths (1.02 cmol$_c$ dm^{-3}). The effective cation exchange capacity (t) showed a similar behavior, oscillating around 1.3–1.5 cmol$_c$ dm^{-3} up to 0.60 m, dropping to 1.02 cmol$_c$ dm^{-3} in the deepest layer.

Base saturation (V%) remained above 57 % in layers up to 1.00 m, indicating soils with moderate chemical fertility. In the 1.00–2.00 m layer, there was a reduction to 53.9 %, evidencing the cumulative effect of acidification and the lower presence of basic cations.

Organic matter (OM) showed the highest levels at the surface (6.7 g kg^{-1} in the 0.00–0.05 m layer), with a continuous reduction until reaching only 1.3 g kg^{-1} at 1.00–2.00 m, a typical pattern of soils with biological activity concentrated in the upper layers.

For unaffected soils (Table 5), coarse sand presents high values in the surface layers (302.4 g kg^{-1} in 0.00-0.15 m), decreasing progressively to 230 g kg^{-1} at a depth of 1.00-2.00 m, indicating a reduction with depth. Fine sand content showed little variation along the soil profile, with similar values in surface and subsurface layers, ranging from 149.5 to 180 g kg^{-1}. Silt remains stable in the upper layers (147.7-150.6 g kg^{-1}), but reduces abruptly to 10 g kg^{-1} at maximum depth. Clay increases gradually with depth, from 371.7 g kg^{-1} at 0.00-0.30 m to 580 g kg^{-1} at 1.00-2.00 m, indicating a higher concentration of fine particles at depth.

Unaffected soils presented chemical properties typical of naturally acidic and low-fertility environments. The pH(H_2O) varied from 5.5 at the surface (0.00–0.15 m) to 4.54 in the deepest layer (1.00–2.00 m), indicating increasing acidity with depth. Available phosphorus levels were low throughout the profile (<2 mg dm^{-3}), which is common in highly weathered soils. Potassium levels also showed a sharp decline with depth, going from 47 mg dm^{-3} at the surface to only 2 mg dm^{-3} in the 1.00-2.00 m layer.

Sum of bases (SB) and the effective cation exchange capacity (t) followed a similar trend, with values decreasing in the deepest layers. Base saturation (V%) was low throughout the profile, ranging from 25.4 to 40.45 %, except in the deepest layer, where it fell to 9.3 %, reflecting the low natural fertility of these soils. Organic matter (OM) content was higher in the surface layers (25.5 g kg^{-1} up to 0-0.15 m), decreasing progressively with depth until reaching 12.05 g kg^{-1} at 0.60-1.00 m.

Kruskal-Wallis test (Table 6) revealed statistically significant differences ($p<0.0001$) between the soil groups (Technosols, tailings and unaffected soils) for most of the chemical variables evaluated. In general, the Technosols presented higher pH and higher available phosphorus (P) contents throughout the profile, especially in the surface layers (Figure 6), while the unaffected soils showed greater availability of potassium (K), greater sum of bases (SB), effective CTC (t) and organic matter (OM) contents, especially up to 0.30 m in depth. Base saturation (V%) was more stable and higher in the Technosols.

Multivariate data analysis

The analysis of Spearman's correlation between silt and other soil parameters reveals that there is a weak relationship between P (phosphorus availability) (0.43), pH (0.47) and base saturation (0.40). Clay, in turn, presented a moderate correlation with aluminum (0.52), and a weak relationship with Mg^{2+} and effective CEC (t), with values of 0.33 and 0.37, respectively. Among the chemical properties of the soil, a positive correlation (0.53) was identified between phosphorus and pH. Organic matter presented a high correlation with H+Al and CEC (T). The CEC (T) presented a high correlation with both Mg^{2+}.

Principal Component Analysis (Figures 8 and 9) was used to identify the structure of the relationships between variables under study, condensing complex information into a few interpretable dimensions. Five dimensions were obtained from the variables originally used. Dimension 1 explained 33 % of the data variability, from the largest contribution of the components water pH (-0.53), Mg^{2+} (0.68), Al^{3+} (0.59), H+Al (0.89), t and T (0.67 and 0.94), V% (-0.56), MO (0.61), P rem (-0.57) and Clay (0.75). This indicates that this dimension is related to the presence of organic matter, soil acidity and clay. These variables are more correlated to soils without the presence of tailings, with higher Aluminum, Organic Matter and Clay contents.

Dimension 2 explained 20 %, presents positive correlations with water pH (0.53), available P contents, Ca^{2+}, effective CEC and base saturation, indicating that this dimension may be related to phosphorus availability and soil acidity. Dimension 3 presents a moderate positive correlation with P-rem (-0.50) and Fine sand (-0.62) and Silt (0.64), suggesting that there is a reduction in P-rem with the increase in silt. This dimension was more related to the key characteristics described for the tailings.

Table 5. Median chemical and physical properties values across soil layers for non-affected soils

Layer	pH	P	K	SB	t	V	MO	Coarse sand	Fine sand	Silt	Clay
m	-	mg dm^{-3}		cmol$_c$ dm^{-3}		%	g kg^{-1}				
0.00-0.05	5.5	1.5	47	2.58	2.68	35.1	25.5	302.4	178.2	147.7	371.7
0.05-0.15	5.5	1.5	44	2.52	2.64	29.3	25.5	302.4	178.2	147.7	371.7
0.15-0.30	5.33	1.3	26	1.56	2.04	25.4	21.5	302.1	171.9	145.8	380.2
0.30-0.60	5.2	1.0	16	1.22	1.79	30.9	17.5	271.1	160.1	150.6	418.2
0.60-1.00	5.16	0.9	11	1.16	1.71	40.4	12.0	242.3	149.5	134.0	474.2
1.00-2.00	4.54	0.9	2	0.33	1.20	9.3	NA	230.0	180.0	10.0	580.0

P: available phosphorus (mg dm^{-3}); K: exchangeable potassium (mg dm^{-3}); SB: sum of bases (cmol$_c$ dm^{-3}); t: effective cation exchange capacity (cmol$_c$ dm^{-3}); V: base saturation (%); MO: organic matter (g kg^{-1}); coarse sand, fine sand, silt, and clay (g kg^{-1}).

Table 6. Statistical comparison of soil chemical properties using the Kruskal-Wallis test

Variable	Units	Kruskal-Wallis	Technosols	Tailings	Unaffected soils
pH(H_2O)	-	**<0.0001**	6.4b	7.39c	5.33a
P	mg dm^{-3}	**<0.0001**	4.7b	7.6b	1.3a
K	mg dm^{-3}	**<0.0001**	17b	10c	27a
Na^+	$cmol_c$ dm^{-3}	0.074	0a	0a	2a
Ca^{2+}	$cmol_c$ dm^{-3}	0.397	1.17a	0.87a	0.99a
Mg^{2+}	$cmol_c$ dm^{-3}	**<0.0001**	0.18a	0.06a	0.38b
Al^{3+}	$cmol_c$ dm^{-3}	**<0.0001**	0a	0a	0.1b
H_Al	$cmol_c$ dm^{-3}	**<0.0001**	1.1a	0.3a	3.63b
SB	$cmol_c$ dm^{-3}	**<0.0001**	1.24a	0.95a	1.46b
t	$cmol_c$ dm^{-3}	**<0.0001**	1.53a	0.95a	1.95b
T	$cmol_c$ dm^{-3}	**<0.0001**	2.64a	1.45a	5.82b
V	%	**<0.0001**	59.5a	79.6a	33.8b
m	%	**<0.0001**	0a	0a	3.3b
MO	g kg^{-1}	**<0.0001**	4.0a	0a	19.5b
P_{rem}	mg L^{-1}	**<0.0001**	35.3a	38.8a	25.2b

Medians (P50) of the chemical properties of Technosols, tailings layers and unaffected soils, with significance values from the Kruskal-Wallis test. Equal letters in the same row indicate that there is no statistically significant difference between the groups, according to Dunn's multiple comparisons test (p<0.05).

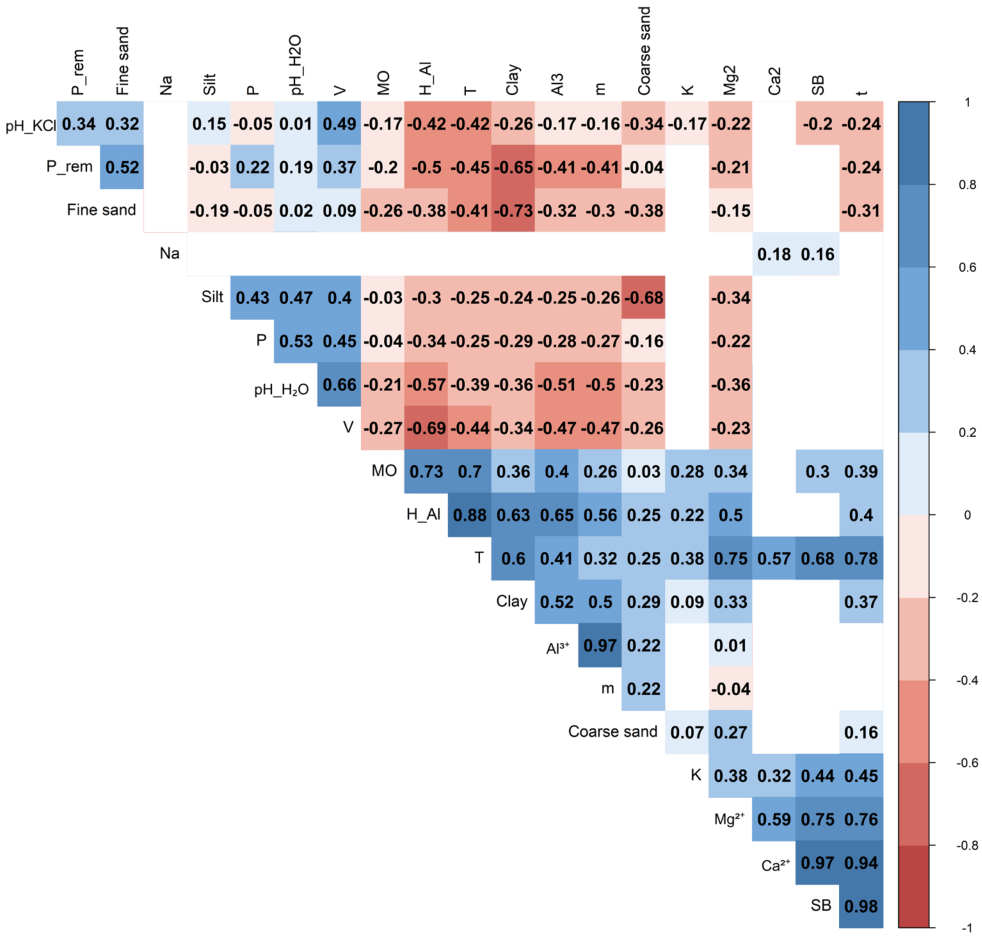

Figure 8. Spearman correlation for the physical and chemical properties of Technosols.

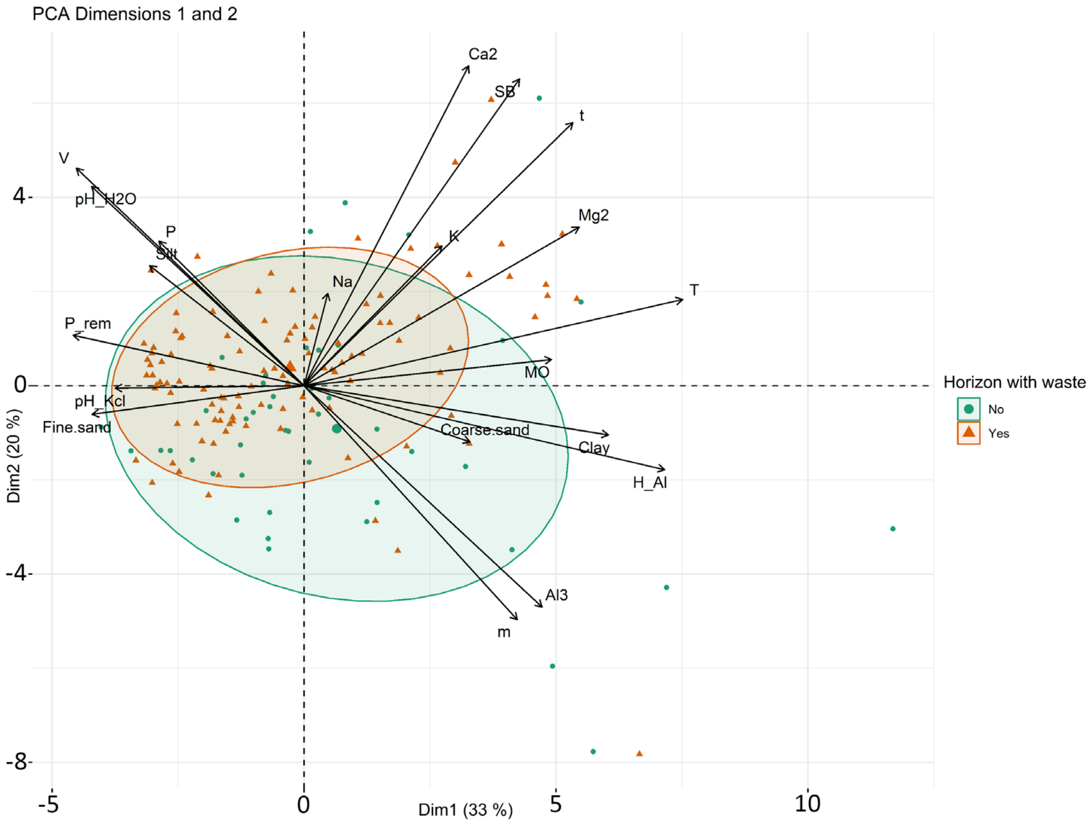

Figure 9. Principal Component Analysis (PCA) based on soil physical and chemical properties. The X-axis represents the first principal component (PC1) and the Y-axis represents the second principal component (PC2), discriminating soil layers with and without tailings.

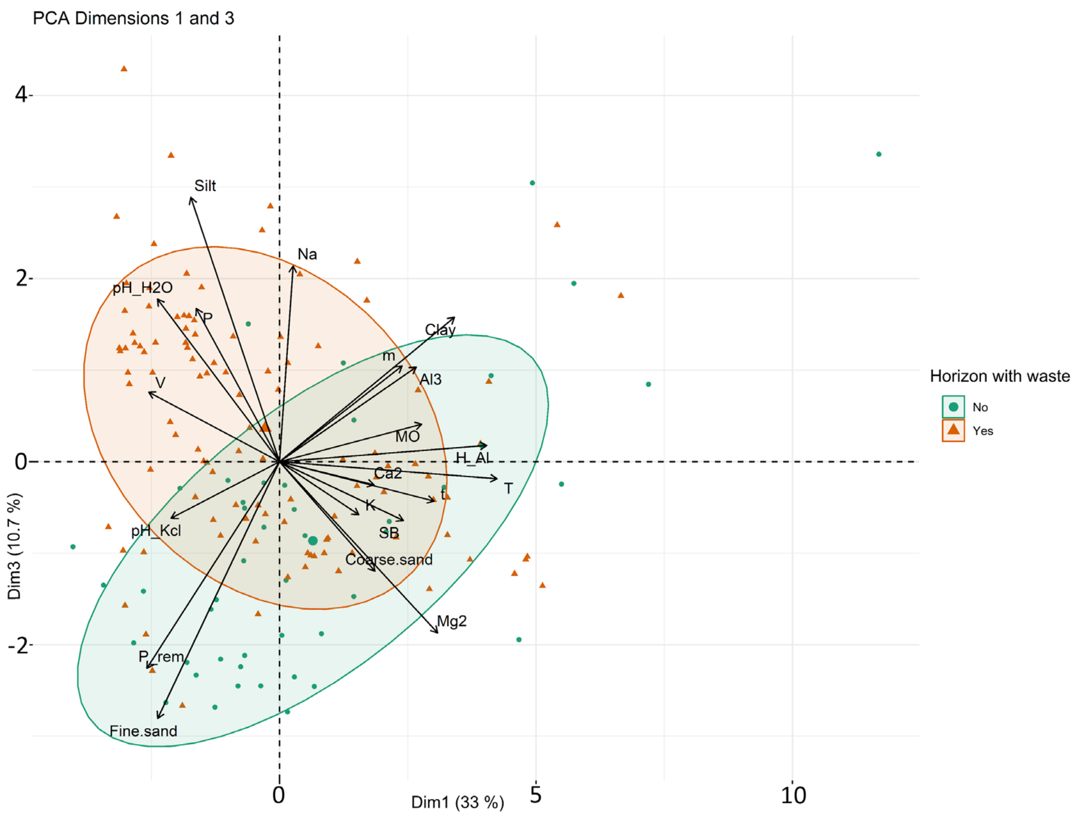

Figure 10. Principal Component Analysis (PCA) based on soil physical and chemical properties. The X-axis represents the first principal component (PC1) and the Y-axis represents the third principal component (PC3), discriminating soil layers with and without tailings.

DISCUSSION

In general, the soils evaluated along the Gualaxo do Norte River presented relatively similar chemical and physical properties, reflecting the homogeneity of the deposited material and the dispersion pattern of the tailings along the geomorphological gradient. Despite this uniformity, subtle variations in position within the landscape and tailings layer thickness were observed. The upstream sectors showed greater deposition variability, possibly associated with higher river energy and channel instability, while the lower sector showed more regular profiles, favored by the lower slope and greater sediment retention capacity.

In the lower stretch of the river, the tailings flow was already mixed with the eroded material from the upstream slopes, which resulted in higher levels of coarse sand and clay in the surface layers of the profiles in sector 3. In this area, the soils in group 3 presented higher levels of calcium, magnesium and organic matter, suggesting less direct influence of the tailings or greater participation of natural materials. These properties contributed to an increase in the sum of bases and cation exchange capacity, indicating soils with better chemical balance. Even at low levels, the presence of organic matter may be associated with residual vegetation or the beginning of natural recomposition processes, positively influencing nutrient retention and soil structure.

The granulometric analysis of the Technosols reveals a typical pattern of recent deposition, with a predominance of fine particles (fine sand and silt) in the surface layers and an increase in coarse sand and clay with depth. This pattern indicates suspended deposition of lighter particles, followed by deposition of heavier materials in the lower layers, as the flow energy decreased throughout the event. The slight increase in clay at depth may be associated with the presence of pre-existing soil horizons or the vertical migration of fine particles over time.

In unaffected soils, a textural profile characteristic of highly weathered environments is observed. The gradual reduction of coarse sand and the increase in clay with depth indicate processes of eluviation/iluvation or pedogenetic differentiation. The sudden reduction of silt in the deeper layers and the slight increase in fine sand may be related to changes in the parent material or to ancient river deposition processes. From a chemical point of view, the Technosols presented a higher pH in the surface layers, reflecting the presence of alkali-rich tailings, such as NaOH used in ore processing. This increase in pH reduces the natural acidity of the soils and favors greater availability of phosphorus, either by direct release of the element or by reduced adsorption in less acidic environments. At depth, pH and available phosphorus decrease, revealing a lesser influence of the tailings and a predominance of the region's natural soil properties, characterized by high acidity and strong phosphorus retention by iron and aluminum oxides. Organic matter was concentrated in the surface layers, which reinforces the role of biological activity in maintaining fertility in these horizons.

In unaffected soils, the chemical data reflect a typical profile of intensely weathered tropical soils, with increasing acidity and decreasing fertility with depth. The lower pH in the lower horizons is common in Oxisols and Ultisols under native vegetation, and is associated with the leaching of bases and accumulation of aluminum. The low phosphorus levels throughout the profile confirm the natural limitation of this nutrient, strongly adsorbed by oxyhydroxides. The reduction in potassium levels, the sum of bases and the effective CEC with depth reinforces the dystrophic character of the subsurface horizons, evidencing the low natural fertility of these soils.

CONCLUSIONS

The collapse of the Fundão dam led to significant changes in the physical and chemical properties of the soils affected along the Gualaxo do Norte River, particularly in the surface layers. The distribution of the tailings reflected the geomorphological gradient of the basin, with greater heterogeneity of deposition in the upper reaches and greater uniformity in the ower sectors, downstream. From a physical point of view, the Technosols presented a greater proportion of fine particles in the upper layers, indicative of tailings deposition with depth, a progressive increase in coarse sand and clay was observed, possibly related to the presence of unaffected horizons or the transition to the alluvial material. Chemically, the impacted soils exhibited higher pH and slight enrichment in phosphorus, sodium, and potassium at the surface, in contrast to the unaffected soils, which showed more pronounced acidity and low fertility throughout the entire profile. Despite the greater variability found in the soils of Sector 3, most of the evaluated profiles displayed similar behavior, indicating relative homogeneity in the soil response to tailings deposition. Nevertheless, the influence of the tailings on fertility is limited to the surface layers and may have implications for environmental recovery and future land use. The natural properties of the studied Technosols indicate the potential for promoting consistent recovery aimed at agricultural or pastoral uses, with low-impact in situ interaction.

SUPPLEMENTARY DATA

Supplementary data to this article can be found online at https://www.rbcsjournal.org/wp-content/uploads/articles_xml/1806-9657-rbcs-50-spe1-e0250071/1806-9657-rbcs-50-spe1-e0250071-suppl01.

DATA AVAILABILITY

The data will be provided upon request.

ACKNOWLEDGEMENTS

This study was carried out with the support of the Coordination for the Improvement of Higher Education Personnel – Brazil (CAPES) - Financing Code 001. To Fundação Renova for providing the data used in this study.

AUTHOR CONTRIBUTIONS

Conceptualization: Anderson Almeida Pacheco (equal), Carlos Ernesto Gonçalves Reynaud Schaefer (equal), Eliana Elizabeth dos Santos (equal), Elpidio Inácio Fernandes Filho (equal), Márcio Rocha Francelino (equal) and Pedro Henrique Araújo Almeida (equal).

Data curation: Carlos Ernesto Gonçalves Reynaud Schaefer (equal), Eliana Elizabeth dos Santos (equal), Márcio Rocha Francelino (equal) and Pedro Henrique Araújo Almeida (equal).

Formal analysis: Anderson Almeida Pacheco (equal), Anifo Ibraimo (equal), Carlos Ernesto Gonçalves Reynaud Schaefer (equal), Elpidio Inácio Fernandes Filho (equal), Márcio Rocha Francelino (equal) and Pedro Henrique Araújo Almeida (equal).

Funding acquisition: Anderson Almeida Pacheco (lead).

Investigation: Anifo Ibraimo (equal), Carlos Ernesto Gonçalves Reynaud Schaefer (supporting), Eliana Elizabeth dos Santos (equal), Elpidio Inácio Fernandes Filho (equal), Márcio Rocha Francelino (equal) and Pedro Henrique Araújo Almeida (equal).

Methodology: Anderson Almeida Pacheco (equal), Elpidio Inácio Fernandes Filho (equal), José Alexandre Melo Demattê (equal), Márcio Rocha Francelino (equal) and Pedro Henrique Araújo Almeida (equal).

Software: Elpidio Inácio Fernandes Filho (equal) and Pedro Henrique Araújo Almeida (equal).

Supervision: Márcio Rocha Francelino (lead).

Validation: Anderson Almeida Pacheco (equal) and Márcio Rocha Francelino (equal).

Writing – original draft: Anderson Almeida Pacheco (equal), Carlos Ernesto Gonçalves Reynaud Schaefer (equal), Eliana Elizabeth dos Santos (equal), Elpidio Inácio Fernandes Filho (equal), José Alexandre Melo Demattê (equal), Márcio Rocha Francelino (equal) and Pedro Henrique Araújo Almeida (equal).

Writing – review & editing: Anderson Almeida Pacheco (equal), Anifo Ibraimo (equal), Carlos Ernesto Gonçalves Reynaud Schaefer (equal), Eliana Elizabeth dos Santos (equal), Elpidio Inácio Fernandes Filho (equal), José Alexandre Melo Demattê (equal), Márcio Rocha Francelino (equal) and Pedro Henrique Araújo Almeida (equal).

REFERENCES

Alvarez V VH, Ribeiro AC, Ribeiro AC, Guimarães PTG. Recommendations for the Use of Soil Amendments and Fertilizers in Minas Gerais: 5th Approximation. In: Alvarez VVH, editor. Soil Fertility Commission of the State of Minas Gerais – CFSEMG. Minas Gerais: Viçosa; 1999. p. 359.

Alvarez V VH, Novais RF, Dias LE, Oliveira JA. Determinação e uso do fósforo remanescente. In: Sociedade Brasileira de Ciência do Solo - SBCS. Boletim Informativo da Sociedade Brasileira de Ciência do Solo. 2000;25:25-37.

Agência Nacional de Mineração - ANM. Informe Mineral 04TRI2023. Brasília, DF: ANM; 2023. Available from: https://www.gov.br/anm/pt-br/assuntos/economia-mineral/publicacoes/informe-mineral/publicacoes-nacionais/informe04tri2023.pdf.

Andrade LCR. Caracterização de rejeitos de mineração de ferro, *in natura* e segregados, para aplicação como material de construção civil [thesis]. Viçosa, MG: Universidade Federal de Viçosa; 2014.

Arrouays D, McBratney A, Minasny B, Hempel J, Heuvelink G, MacMillan R, Hartemink A, Lagacherie P, McKenzie N. The GlobalSoilMap project specifications. In: Arrouays D, McKenzie N, Hempel J, Forges AR, McBratney A, editors. GlobalSoilMap: Basis of the global spatial soil information system. Boca Raton: CRC Press; 2014. p. 9-12.

Beaudette DE, Roudier P, O'Geen AT. Algorithms for quantitative pedology: A toolkit for soil scientists. Comput Geosci. 2013;52:258-68. https://doi.org/10.1016/j.cageo.2012.10.020

Beaudette DE, Skovlin J, Brown AG, Roudier P, Roecker SM. Algorithms for quantitative pedology. In: Zinck JA, Metternicht G, del Valle HF, Angelini M, editors. Geopedology: An integration of geomorphology and pedology for soil and landscape studies. Cham: Springer International Publishing; 2023. p. 201-22. https://doi.org/10.1007/978-3-031-20667-2_11

Carmo FF, Kamino LHY, Tobias Junior R, Campos IC, Carmo FF, Silvino G, Castro KJSX, Mauro ML, Rodrigues NUA, Miranda MPS, Pinto CEF. Fundão tailings dam failures: The environmental tragedy of the largest technological disaster of Brazilian mining in global context. Perspect Ecol Conserv. 2017;15:145-51. https://doi.org/10.1016/j.pecon.2017.06.002

Carvalho PSL, Silva MM, Rocio MAR, Moszkowicz J. Minério de Ferro. In: Biblioteca digital – BNDES. Rio de Janeior: BNDES Setorial; 2014. p. 197-233. Available from: http://web.bndes.gov.br/bib/jspui/handle/1408/4802.

Dorr II JVN. Physiographic, stratigraphic, and structural development of the Quadrilátero Ferrífero, Minas Gerais, Brazil. Washington, DC: Geological Survey Professional; 1969. (Paper 641-A). https://doi.org/10.3133/pp641A

Dorr II JVN, Gair JH, Pomerene JB, Rynearson GA. Revisão estratigráfica precambriana do Quadrilatero Ferrífero, Brasil. Departamento Nacional da Produção Mineral; 1957.

Duarte EB, Neves MA, Oliveira FB, Martins ME, Oliveira CHR, Burak DL, Rangel CVGT. Trace metals in Rio Doce sediments before and after the collapse of the Fundão iron ore tailing dam, Southeastern Brazil. Chemosphere. 2021;262:127879. https://doi.org/10.1016/j.chemosphere.2020.127879

Felippe MF, Mendes LC. Para onde foi a lama da barragem de Fundão (Mariana, Minas Gerais)? A distribuição dos rejeitos ao longo dos vales fluviais afetados pelo desastre da Samarco/Vale/BHP. Rev Espinhaço. 2022;11:1-14. https://doi.org/10.5281/zenodo.5883450

Gair JE. Age of gold mineralization at the Morro Velho and Raposos mines, Minas Gerais. Bol Soc Bras Geol. 1958;7:39-45.

Guerra MBB, Teaney BT, Mount BJ, Asunskis DJ, Jordan BT, Barker RJ, Santos EE, Schaefer CEGR. Post-catastrophe analysis of the Fundão Tailings dam failure in the Doce River system, Southeast Brazil: Potentially toxic elements in affected soils. Water Air Soil Pollut. 2017;228:252. https://doi.org/10.1007/s11270-017-3430-5

Hongyu K, Sandanielo VLM, Oliveira Junior GJ. Análise de componentes principais: Resumo teórico, aplicação e interpretação. E&S Eng Sci. 2016;5:83-90. https://doi.org/10.18607/ES201653398

Husson F, Josse J, Le S, Mazet J. FactoMineR: Multivariate exploratory data analysis and data mining with R. Version 1.35. R package; 2017. Availablre from: https://CRAN.R-project.org/package=FactoMineR.

IUSS Working Group WRB. World reference base for soil resources 2014, update 2015: International soil classification system for naming soils and creating legends for soil maps. Rome: Food and Agriculture Organization of the United Nations; 2015. (World Soil Resources Reports, 106).

Jenny H. Factors of soil formation: a system of quantitative pedology. North Chelmsford: Courier Corporation; 1994.

Köppen W. Climatology with a Study of the Climates of the Earth. Ciudad del México: Fundo de Cultura Econômica; 1948.

Marta-Almeida M, Mendes R, Amorim FN, Cirano M, Dias JM. Fundão Dam collapse: Oceanic dispersion of River Doce after the greatest Brazilian environmental accident. Mar Pollut Bull. 2016;112:359-64. https://doi.org/10.1016/j.marpolbul.2016.07.039

Mehlich A. New extractant for soil test evaluation of phosphorus, potassium, magnesium, calcium, sodium, manganese and zinc. Commun Soil Sci Plant Anal. 1978;9:477-92. https://doi.org/10.1080/00103627809366824

Mendonça ES, Matos ES. Matéria orgânica do solo: Métodos de análises. Viçosa, MG: Universidade Federal de Viçosa; 2005.

Oliveira BTA, Mendes LC, Felippe MF, Silva BM. Fluvial morphology transformations resulting from the Fundão dam collapse: preliminary studies. In: XVII Simpósio Brasileiro de Geografia Física Aplicada, I Congresso Nacional de Geografia Física: Os desafios da Geografia Física na Fronteira do Conhecimento. Campinas: Unicamp; 2017. p. 3941-52. https://doi.org/10.20396/sbgfa.v1i2017.2543

Pinheiro HSK, Chagas CDS, de Carvalho WDJ, Anjos LHCD. Pedometric tools to characterize granulometric composition of hydromorphic soil profiles. Pesq Agropec Bras. 2016;51:1326-38. https://doi.org/10.1590/S0100-204X2016000900032

Pinheiro HSK, Xavier PA, Anjos LHC, Chagas CS, Carvalho Junior W. Quantitative pedology to evaluate a soil profile collection from the Brazilian semi-arid region. S Afr J Plant Soil. 2018;35:269-79. https://doi.org/10.1080/02571862.2017.1419385

R Development Core Team. R: A language and environment for statistical computing. Vienna, Austria: R Foundation for Statistical Computing; 2021. Available from: http://www.R-project.org/.

Renger FE, Noce CM, Romano AW, Machado N. Evolução sedimentar do Supergrupo Minas: 500 Ma. de registro geológico no Quadrilátero Ferrífero, Minas Gerais, Brasil. Geonomos. 1994;2:1-11. https://doi.org/10.18285/geonomos.v2i1.227

Saadi A, Campos JCF. Geomorfologia do caminho da lama: contexto e consequências da ruptura da Barragem do Fundão(novembro 2015, Mariana–MG). Arq Mus Hist Nat Jardim Bot. 2015;11:63-103.

Santos EE. Diagnosis and monitoring of technosols from iron mining tailings of the Fundão dam through remote and proximal soil inspection techniques [thesis]. Viçosa, MG: Universidade Federal de Viçosa; 2019.

Santos RD, Lemos RC, Santos HG, Ker J, Anjos LHC, Shimizu S. Manual de descrição e coleta de solo no campo. 6. ed. Viçosa, MG: Sociedade Brasileira de Ciência do Solo; 2013.

Schaefer CEGR, Santos EE, Fernandes Filho EI, Assis IR. Paisagens de lama: Os tecnossolos para recuperação ambiental de áreas afetadas pelo desastre da barragem do Fundão. In: Sociedade Brasileira de Ciência do Solo - SBCS. Boletim Informativo da Sociedade Brasileira de Ciência do Solo. 2016;42:18-23.

Schaefer CEGR, Santos EE, Souza CM, Neto JD, Fernandes Filho EI, Delpupo C. Cenário histórico, quadro físiográfico e estratégias para recuperação ambiental de Tecnossolos nas áreas afetadas pelo rompimento da barragem do Fundão, Mariana, MG. Arq Mus Hist Nat Jardim Bot. 2015;24:105-35.

Segura FR, Nunes EA, Paniz FP, Paulelli ACC, Rodrigues GB, Braga GUL, Pedreira Filho WR, Barbosa Jr F, Cerchiaro G, Silvs FF, Batista BL. Potential risks of the residue from Samarco's mine dam burst (Bento Rodrigues, Brazil). Environ Pollut. 2016;218:813-25. https://doi.org/10.1016/j.envpol.2016.08.005

Silva AO, Guimarães AA, Lopez BDO, Zanchi CS, Veja CFP, Batista ER, Moreira FMS, Souza FRC, Pinto FA, Santos JV, Carneiro JJ, Siqueira JO, Kemmelmeier K, Guilherme LRG, Rufini M, Dias Junior MS, Aragão OOS, Borges PHC, Oliveira-Longatti SM, Carneiro MAC. Chemical, physical, and biological attributes in soils affected by deposition of iron ore tailings from the Fundão Dam failure. Environ Monit Assess. 2021;193:462. https://doi.org/10.1007/s10661-021-09234-4

Spier CA, Oliveira SM, Sial AN, Rios FJ. Geochemistry and genesis of the banded iron formations of the Cauê Formation, Quadrilátero Ferrífero, Minas Gerais, Brazil. Precambrian Res. 2007;152:170-206. https://doi.org/10.1016/j.precamres.2006.10.003

Teixeira PC, Donagemma GK, Fontana A, Teixeira WG. Manual de métodos de análise de solo. 3. ed. rev e ampl. Brasília, DF: Embrapa; 2017.

United States Salinity Laboratory Staff - USSL STAFF. Diagnosis and improvement of saline and alkali soils. Washington, DC: U.S. Department of Agriculture; 1954. (Handbook 60).

Villa PM Martins SV, Pilocelli A, Kruschewsky GC, Dias AA, Nabeta FH. Attributes of stand-age-dependent forest determine Technosol fertility of Atlantic forest re-growing on mining tailings in Mariana, Brazil. J For Res. 2022;33:103-16. https://doi.org/10.1007/s11676-021-01359-z

Wei T, Simko VR, Levy M, Xie Y, Jin Y, Zemla J. Package "corrplot": Visualization of a correlation matrix. Repository CRAN; 2017. Available from: https://github.com/taiyun/corrplot.

Weiss A. Topographic position and landforms analysis. Seatle: The Nature Conservancy; 2001. Available from: https://env761.github.io/assets/files/tpi-poster-tnc_18x22.pdf.

Wolff AP. Caracterização de rejeitos de minério de ferro de minas da Vale. [thesis]. Ouro Preto: Universidade Federal de Ouro Preto; 2009.